Simplification of Complex EPR Spectra by Cepstral Analysis

Ranjan Das,[†] Michael K. Bowman,[‡] Haim Levanon,[§] and James R. Norris, Jr.*,[||]

Tata Institute of Fundamental Research, Homi Bhabha Road, Mumbai 400005, India, Pacific Northwest National Laboratory, Environmental and Molecular Sciences Laboratory, Richland, Washington 99353, Department of Physical Chemistry, The Hebrew University of Jerusalem, Jerusalem 91904, Israel, and Department of Chemistry, Institute for Biophysical Dynamics, The University of Chicago, Chicago, Illinois 60637

Received: September 26, 2006; In Final Form: March 15, 2007

As the Fourier transform of time-series data is known as the spectrum, the Fourier transform of the logarithm of the time-series data is called the cepstrum of the data. When cepstral analysis is applied to free induction decay signals of free radicals showing first-order EPR spectra, the identification of nuclear hyperfine coupling constants becomes simple. In a systematic manner, we have examined how the technique of cepstral analysis is affected by the presence of aliasing, noise, uncertainty in the time origin of the free induction decay, the presence of second-order hyperfine couplings, and the applications of various apodization methods. This technique was then applied to analyze the EPR spectrum of anthraquinone anion radical, and anion radicals of porphycene and tetrapropyl-porphycene, and the hyperfine coupling constants thus obtained were compared with published data. A good agreement was always found. We make a case for the usefulness of cepstral analysis in determining the hyperfine coupling constants of complex EPR spectra of organic free radicals.

Introduction

Large organic free radicals, such as those found in photosynthetic model systems, often have very complex EPR spectra with hundreds of hyperfine lines arising from the large number of magnetic nuclei interacting with the unpaired electron. ENDOR spectroscopy is often used to measure the hyperfine couplings in such cases, but it requires special temperature and solvent conditions, and also determination of the number of equivalent nuclei by ENDOR is problematic. The EPR spectrum is a convolution of all the hyperfine splittings and contains a great deal of redundant information. When good resolution can be obtained in the EPR spectrum, it should be possible to measure both the hyperfine couplings and the number of equivalent nuclei from the regularities in the shape of the EPR spectrum.

One approach to the simplification of EPR spectra is to use a pattern recognition method to identify the hyperfine couplings and simplify the EPR spectrum. Such a method is the cepstral analysis developed by Bogert et al.[1] It was first applied to the analysis of earthquake data[1] and later applied by Kirmse[2] to EPR spectra. The name *cepstrum* is an anagram of the well-known term *spectrum*. A cepstrum is somewhat reminiscent of the spectrum from the ENDOR technique of special TRIPLE.[3]

Pearson et al.[4] tried to use cepstral analysis on the EPR spectra of substituted triarylaminium cation radicals and concluded that, in practice, this technique was not very useful. We find, in contrast, that when the basic axioms of the method are met, cepstral analysis can be a very effective aid in the analysis of complex hyperfine spectra obtained from photosynthetic model compounds such as the anion radicals of synthesized porphycenes.[5] As long as the EPR spectra are well-resolved, cepstral analysis can provide recognizable patterns in an EPR spectrum, thus allowing for the identification of the hyperfine couplings, as well as providing some information about the number of equivalent nuclei.

In this paper, we first examine the effect of noise, nonuniform line width, and aliasing on the cepstrum using simulated data. We then analyze EPR spectra taken by both Fourier-transform EPR and CW-EPR methods. The hyperfine coupling constants obtained using the cepstral analysis are in agreement within 50−80 kHz (∼2−4%) when compared to ENDOR-derived couplings. The cepstral analysis is very effective without requiring the special operating conditions needed for ENDOR.

Method

The time domain free induction decay of EPR signals corresponding to *m* spin-1/2 nuclei and *n* spin-1 nuclei is given as[2,6]

$$y(t) = R(t)\prod_{i=1}^{m}\cos(\pi\nu_i t)\prod_{j=1}^{n}(1 + 2\cos(2\pi\nu_j t)) \qquad (1)$$

when second-order shifts and nuclear spin-dependent relaxation effects are negligible. Here $R(t)$ is the decay function and is assumed to be same for all the nuclei, $2\nu_i$ is the coupling constant of a spin-1/2 nucleus, and $2\nu_j$ is that of a spin-1 nucleus. Since such nuclei are commonly encountered in organic free radicals, we have examined only these nuclei here. Generalization to nuclei of any spin is easy and has been done by Kirmse.[2] The indices *m* and *n* include possible degeneracies such that ν_1 and ν_2, for example, are not necessarily distinct.[6]

* Corresponding author. Phone: 773-702-7864. Fax: 773-702-9646. Email: j-norris@uchicago.edu.
[†] Tata Institute of Fundamental Research.
[‡] Pacific Northwest National Laboratory, Environmental and Molecular Sciences Laboratory.
[§] The Hebrew University of Jerusalem.
[||] The University of Chicago.

10.1021/jp066327p CCC: $37.00 © 2007 American Chemical Society
Published on Web 05/08/2007

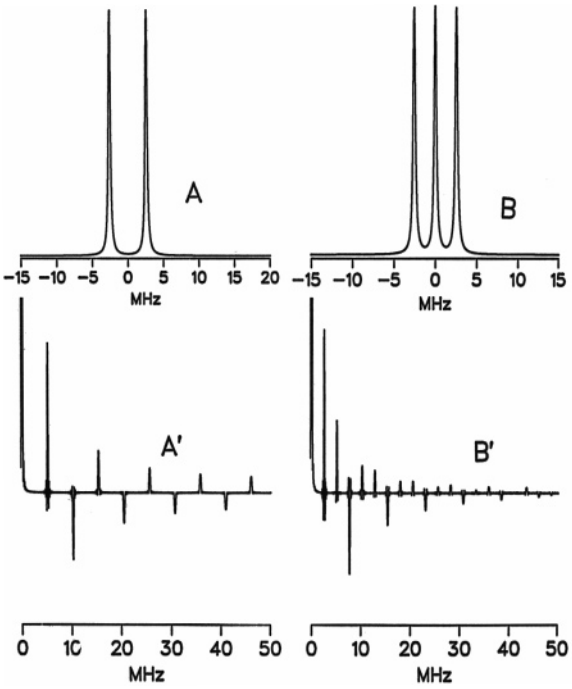

Figure 1. Comparison of EPR spectra with hyperfine coupling of 5 MHz to a spin-1/2 nucleus (A) and of 2.5 MHz to a spin-1 nucleus (B). A′ and B′ show the corresponding cepstra. The FIDs were generated using 2048 points with a sampling interval of 10 ns.

Taking the logarithm of the absolute value of $y(t)$ we get

$$\ln |y(t)| = \ln |R(t)| + \sum_i \ln |\cos(\pi \nu_i t)| + \sum_j \ln |1 + 2\cos(2\pi \nu_j t)| \quad (2)$$

which shows that all the coupled nuclei have been decoupled and each can be examined independently of the others. Fourier transformation of eq 2 generates the cepstrum as

$$F \ln |y(t)| = F \ln |R(t)| + \sum_i F \ln |\cos(\pi \nu_i t)| + \sum_j F \ln |1 + 2\cos(2\pi \nu_j t)| \quad (3)$$

The transform of the line shape function $R(t)$ will be nonzero near zero frequency; except for nuclei with very small coupling constants, this zero frequency signal will not affect the rest of the cepstrum. The role of $R(t)$ will not be considered in further discussion.

Spin-1/2 Nuclei. Since the logarithm of the absolute value of a cosine function is given as[7]

$$\ln |\cos x| = -\ln 2 + \cos 2x - (\cos 4x)/2 + (\cos 6x)/3 - \ldots$$

we see that

$$F \ln |\cos(\pi \nu t)| = -\ln 2\delta(0) + \sum_k (-1)^{k+1}[\delta(\omega - 2\pi k\nu)]/k \quad (4)$$

which shows, except for the peak at zero frequency, a series of peaks with alternating signs and decreasing magnitude, each separated by the coupling constant 2ν.

Spin-1 Nuclei. Expressing $1 + 2\cos(2\pi\nu t)$ as $(\sin(3\pi\nu t))/\sin(\pi\nu t)$, we find

$$F \ln |1 + 2\cos(2\pi \nu t)| = F \ln |\sin(3\pi \nu t)| - F \ln |\sin(\pi \nu t)| = \sum_k \delta(\omega - 2\pi\nu k)/k - \sum_l \delta(\omega - 6\pi\nu l)/l \quad (5)$$

The cepstrum given by eq 5 is again a series of peaks separated by the coupling constant 2ν. But in contrast to eq 4, a pair of positive peaks is followed by a negative peak, which is followed by another pair of positive peaks, and so on. In general, for a spin-I nucleus, the cepstrum consists of $2I$ positive peaks, followed by one negative peak, and the pattern repeats. So by identifying the pattern of the harmonics of a coupling constant, the spin of the nucleus can be readily identified.

Figure 1 shows cepstra of spin-1/2 and spin-1 nuclei generated from a synthesized free induction decay signal. The cepstral peaks have finite width resulting from the limited frequency bandwidth (governed by the Nyquist frequency) and the finite number of data points in the time domain data. Nevertheless, the fact that the line shape function of the EPR spectrum does not appear in the cepstral peaks makes identification of line positions relatively easy.

Of considerable significance of a cepstrum is that the location of one cepstral line and its harmonics solely depends on the coupling constant of the particular nucleus and is independent of the coupling constants of other nuclei, a direct consequence of eq 2. The situation is quite different for CW EPR where the position of each hyperfine line is a function of all the hyperfine couplings and the number of magnetic nuclei. This property of the cepstrum is similar to ENDOR spectroscopy and is particularly useful in identifying various coupling constants in a simple and systematic way.

Potential Problems of Cepstral Analysis. *(1) Aliasing or Folding-Over.* As the cepstrum contains many harmonics of the hyperfine coupling ν, some of them may be aliased, that is, "folded over", to a frequency ν_A, such that $\nu_A = |2N\nu_{Ny} - \nu| \leq \nu_{Ny}$, where ν_{Ny} is the Nyquist frequency and N is an integer. Whether the folded-over peaks will appear in practice is dependent upon the intensity which is inversely proportional to the harmonic number k or l in eqs 4 and 5. Figure 2A shows the cepstrum of an EPR signal with a spin-1 coupling constant of 15 MHz. One can identify the peaks at 15, 30, and 45 MHz that have the characteristic pattern of a spin-1 nucleus. There are, however, more lines with appreciable intensities. The ν_{Ny} for this spectrum was 50 MHz. Therefore, the fourth harmonic ($k = 4$ in eq 5) of the cepstrum which should have appeared at 60 MHz is aliased to 40 MHz. In fact, the peaks at 40, 25, and 10 MHz, marked with a ●, have the right intensities as required by the harmonics 4, 5, and 6, respectively. In order to minimize the aliasing, the Nyquist frequency (ν_{Ny}) can be increased by extending the frequency range of the frequency domain signal by zero filling. This was done in the following way. The FID signal corresponding to Figure 2A was first Fourier transformed to the frequency domain in a window covering from −50 to +50 MHz. Then zeroes were added at one end of the spectrum to extend the spectral window to 200 MHz (from −50 to +150 MHz). The FID signal was reconstructed by an inverse Fourier transform, and the cepstrum was generated from this FID (Figure 2B). In this way, ν_{Ny} was increased to 100 MHz, and as expected, the peaks corresponding to harmonics 4, 5, and 6 disappeared, as the aliasing corresponding to those frequencies was removed. The remaining small peaks are aliases from frequencies higher than 100 MHz. Figure 2C shows the cepstrum when the spectral window was increased to 400 MHz and ν_{Ny}

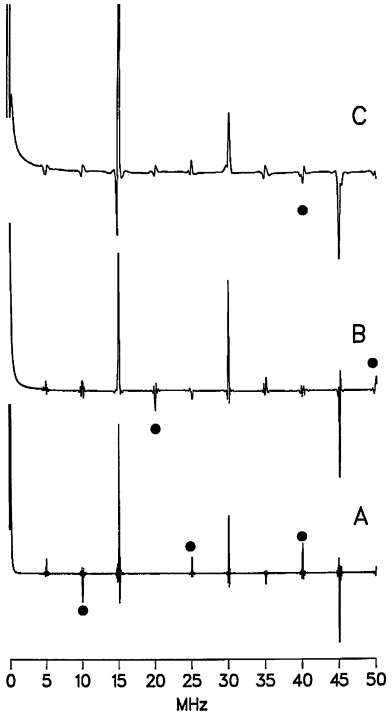

Figure 2. An example of aliasing of a cepstrum with a hyperfine coupling of about 15 MHz to a spin-1 nucleus. The spectral window of (A) was −50 to +50 MHz, and Nyquist frequency ν_{Ny} was 50 MHz. The aliased peaks corresponding to the fourth, fifth, and sixth harmonics are marked with a ●. These aliased peaks were removed in (B) where the spectral window was increased to ±100 MHz, and ν_{Ny} to 100 MHz. Appearance of aliased peaks in (B), marked with a ●, were removed in (C) where the spectral window was increased to ±200 MHz and ν_{Ny} to 200 MHz. (C) has an aliased peak, marked with a ●, of considerably lower intensity, compared to those in (A) and (B).

to 200 MHz. Here the aliased peaks show broadening which is probably due to round-off error.

(2) Effect of Noise. If $y + \Delta y$ is the signal plus the noise amplitude of the FID and the signal-to-noise ratio is greater than 1, as in Figure 3, the logarithm of $|y + \Delta y|$ can be expanded as

$$\ln(|y+\Delta y|) = \ln\left(|y|\cdot\left|1+\frac{\Delta y}{y}\right|\right) = \ln|y| + \ln\left(\left|1+\frac{\Delta y}{y}\right|\right)$$
$$= \ln|y| + \left|\frac{\Delta y}{y} - \frac{1}{2}\left(\frac{\Delta y}{y}\right)^2 + \frac{1}{3}\left(\frac{\Delta y}{y}\right)^3 - \ldots\right|$$
$$\text{when } -1 < \frac{\Delta y}{y} \leq +1, \text{ i.e., that } \left|\frac{y}{\Delta y}\right| \geq 1$$

showing that the relative noise increases as the signal-to-noise approaches 1. Consequently, on taking the logarithm, not only does the signal amplitude decrease, but also the relative noise amplitude increases with the decrease of the signal amplitude. Thus, even though the noise amplitude of the FID is constant over the whole of the recorded signal, the noise in the logarithm of the FID becomes nonuniform. This effect on the signal-to-noise ratio of the logarithm of the signal is most noticeable where the FID signal goes through zero. Figure 3 shows the effect of decreasing the signal-to-noise ratio of a simulated FID and the resulting cepstrum. Note that the increase of noise affects the higher harmonics more than the lower ones. Even though the cepstral peak corresponding to the third harmonic was more intense than the second peak, the deterioration of the signal-to-noise of the third peak was more than that of the second

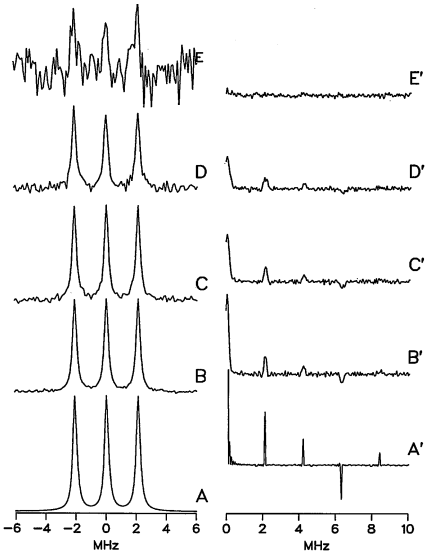

Figure 3. Examples of the effect of decreasing the signal-to-noise ratio of an FID signal on the cepstra. The left panel shows the EPR spectra with a hyperfine coupling to a spin-1 nucleus. These spectra were obtained by the Fourier transform of a synthesized FID signal, to which noise of various magnitudes was added. The maximum magnitude of the noise-free FID was 1. White noise, in the form of uniform random deviates between −1.0 and 1.0, was multiplied by a positive number $f < 1$ and added to this FID signal. The resulting FID signal with noise is designated to have a signal-to-noise ratio of $1/f$. The signal-to-noise ratio of the synthesized FID was the following: (A) no noise, (B) 50, (C) 20, (D) 10, (E) 1.4. The right panel shows the corresponding cepstrum. For all these cepstra, the threshold was set to 0.00001.

peak. The result is that the height of the cepstral peaks does not follow the expected pattern and their phases change. As the noise increases, lower and lower harmonics are affected and eventually no noticeable cepstral peak can be seen.

In order to reduce the noise amplitude in the $\ln|y + \Delta y|$, and consequently, in the resulting cepstrum, we have adopted the following method. We choose a suitable small positive number, T, and call it the threshold. If the magnitude of y is less than T, this magnitude is then set to T. This way only the noise (and the signal) of the FID of magnitude at least equal to T, can contribute to the cepstrum. Since the threshold removes the signal along with the noise, this process affects the cepstral line shapes. Figure 4 shows the effect of increasing the threshold on the cepstrum of a noise-free FID from a spin-1 nucleus of coupling constant of about 2.5 MHz. With the increase in the value of the threshold, the line width of the cepstral peaks increases, the effect being greater on the higher harmonics.

The thresholding may affect the phases of the cepstral peaks as well if the coupling constant is small. For proper identification of signal intensities with correct phases in the frequency domain, the free induction decay oscillations should be recorded over many cycles. The FID of smaller coupling constants has fewer oscillations in a given period of time compared to those of coupling constants of larger value. Consequently the "tail" of the FID is more important for the phase of the signal associated with small coupling constants than for the larger coupling constants. Thresholding may remove much of the signal information from the tail of the FID. The result is that the cepstral peaks for the smaller coupling constants seem to be affected more than the peaks corresponding to larger coupling constants.

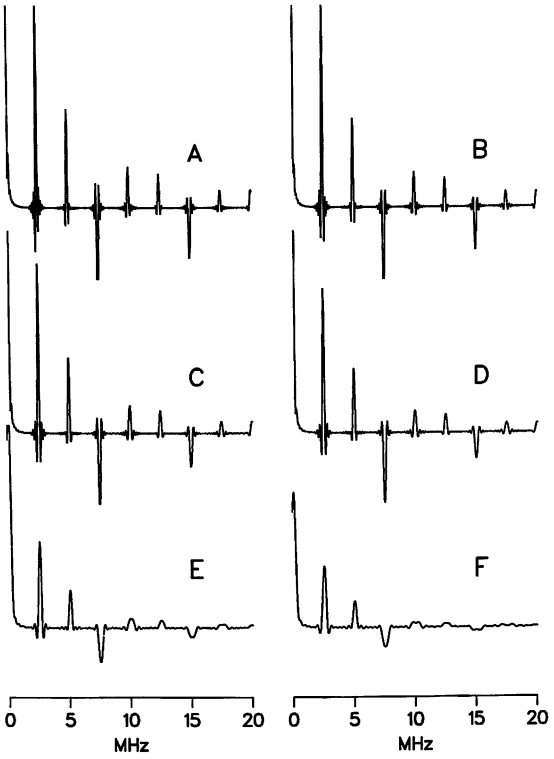

Figure 4. Examples showing the effect of thresholding on the cepstra of a spin-1 nucleus. The FID signal was noise-free, and its maximum value was 1. The threshold was set to 0.001 in (A), 0.002 in (B), 0.005 in (C), 0.01 in (D), 0.05 in (E), and 0.10 in (F).

(3) Effect of the Time Origin of the FID. If the time origin of the FID signal is not correct, the effect in the cepstrum may be understood from the expression of ln $|\cos(\omega t)|$. Replacing t by $t + \Delta t$, we see that

$$\ln|\cos(\omega t + \omega\Delta t)| = -\ln 2 + \cos 2(\omega t + \omega\Delta t) - (\cos 4(\omega t + \omega\Delta t))/2 + (\cos 6(\omega t + \omega\Delta t))/3 \ldots \quad (6)$$

If $\omega\Delta t$ happens to be exactly equal to $\pi/2$, eq 6 becomes

$$\ln|\sin \omega t| = -\ln 2 - \cos 2\omega t - (\cos 4\omega t)/4 - (\cos 6\omega t)/3 - \ldots \quad (7)$$

which shows that *all* the peaks in the cepstrum will be negative. If Δt exhibits a small deviation from zero, its effect will be more noticeable on the higher harmonics. Such a nonzero value of Δt will result when the starting time, $t = 0$, of the FID signal is not accurately known.

(4) Effect of Derivative Signals in the Frequency Domain. The expression for the FID as given by eq 1 is applicable when the signal is recorded in a time-resolved EPR spectrometer not using field modulation or when the 0th derivative absorption spectrum in the frequency domain is transformed to the time domain by inverse Fourier transform. A 0th derivative absorption profile may be obtained by numerical integration of the first derivative EPR signal as typically provided by magnetic field modulation. However, numerical integration is unnecessary for application of cepstral analysis. Let $Y(\omega)$ be the Fourier transform of $y(t)$ and $Y'(\omega) \equiv dY(\omega)/d\omega$ be the experimental spectrum. Since

$$y_1(t) \equiv F^{-1}Y'(\omega) = -it\,y(t) \quad (8)$$

$$\ln|y_1(t)| = \ln|t| + \ln|y(t)| \quad (9)$$

Thus

$$F \ln|y_1(t)| = F \ln|t| + F \ln|y(t)| \quad (10)$$

which shows that the cepstrum of $y_1(t)$ is a superposition of the cepstra of $y(t)$ and t. The cepstrum of t will change the intensities of the cepstral peaks of $y(t)$ to a certain extent. In practice this does not cause so much distortion as to make the identification of peaks difficult.

(5) Effect of Second-Order Couplings and Nonuniform Line Width. The FID of a system in which second-order hyperfine interactions are present will not be represented by eq 1. Nor will the line shape function be represented by a single function $R(t)$. Thus the assumptions of cepstral analysis will no longer hold in such systems. However, when the second-order effects are small, they are not resolved from the first-order lines. The observable effect in such a situation is that the line positions are slightly shifted from the first-order positions and also the width of the outer lines of the spectrum may be more than that of the inner lines. Nuclear spin-dependent relaxation mechanisms also generally make the outer lines broader. In order to see the effect of these on the cepstrum, we have simulated a FID with couplings to three equivalent spin-1/2 nuclei (Figure 5). The frequencies of the two outer lines of the quartet pattern have been changed as well as the line widths. It is seen that both the intensities and phases of the harmonics in the cepstrum are affected and changing the frequency of the outer lines has a more adverse effect than changing the line widths. The limited success of Pearson et al.[4] with the cepstral analysis may be due to the presence of the second-order couplings and low signal-to-noise ratio of the EPR spectrum.

In summary, the identification of the harmonic frequencies will always be useful for precise determination of the coupling constants, but their peak height and phase (alternating positive or negative peaks) may not always be detected with adequate precision. From an experimental cepstrum, starting from the zero frequency, one may choose the very first peak and generate all of its harmonics from a synthesized FID. Comparing with the peaks of the experimental cepstrum, one then strikes out the possible harmonics present in the experimental cepstrum. Then the next higher frequency peak is chosen and its synthesized cepstrum is generated, so as to strike out its harmonics in the experimental spectrum. While generating the synthesized cepstrum, the spin of the nucleus may be chosen to be either 1/2 or 1, so as to match any observed phase of the peaks in the experimental cepstrum. In this process, much like the sieve of Eratosthenes, some possible coupling constants are identified. Then knowing the chemical formula, the observed spectral width of the EPR spectrum, the experimental EPR spectrum, and/or the FID, the right combination of nuclei and the their coupling constants can be established for the best match.

Experimental

The anion radical of anthraquinone radical was prepared photolytically in a solution of 2-butanol/KOH. The free induction decay was recorded by a time-resolved EPR spectrometer.[8−10] The anion radicals of free base porphycene (H_2PC1) and tetrapropyl-porphycene (H_2PC2) in tetrahydrofuran solution were generated by reduction with sodium metal. The CW EPR spectra were recorded in an X-band Bruker model ESP-300 EPR spectrometer using 100 kHz magnetic field modulation.

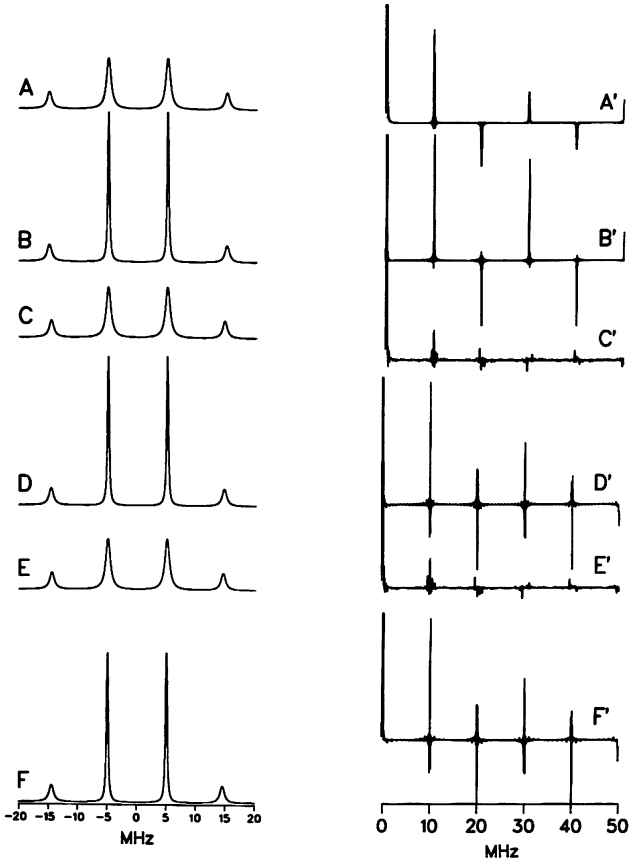

Figure 5. Effect of second-order hyperfine interactions on the cepstra. The left-hand panel shows the EPR spectra with the hyperfine coupling to three equivalent spin-1/2 nuclei. The right panel shows the corresponding cepstra. The spectra were characterized by four variables: (*f*1, *f*2, *k*1, *k*2), where *f*1 is the separation between the inner two lines and *f*2 is that of the outer two lines, and *k*1 and *k*2 are the free induction decay rate constant for the inner two lines and *k*2 is that of the outer two lines. The units of *f*1 and *f*2 are MHz, whereas those of *k*1 and *k*2 are arbitrary. (A) 10, 30, 30, 30; (B) 10, 30, 10, 30; (C) 10, 29.5, 30, 30; (D) 10, 29.5, 10, 30; (E) 10, 29, 30, 30; (F) 10, 29, 10, 30. Note that (A) corresponds to no second-order hyperfine interaction. The synthesized FID signals were noise-free. The spectrum and cepstrum pairs here show that changing the line positions has much more adverse effect on the cepstrum than the change in the line widths.

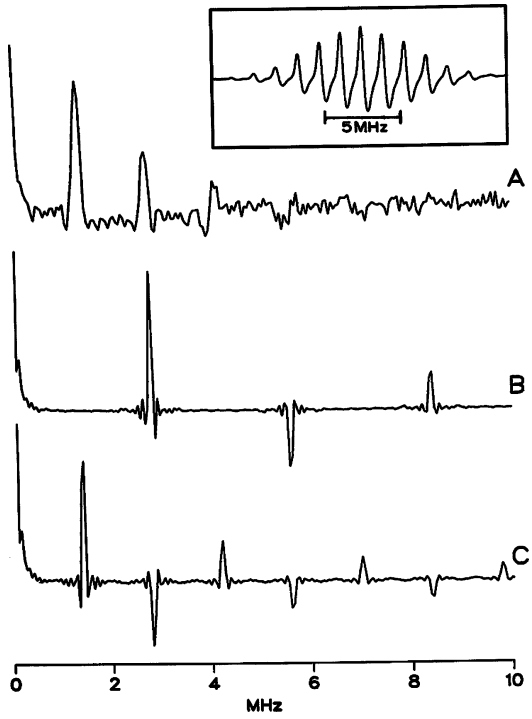

Figure 6. Cepstral analysis of the EPR spectrum of anthraquinone anion radical. The generated cepstrum from the experimental FID is shown in (A), while (B) and (C) show synthesized cepstra with coupling to a spin-1/2 nucleus of coupling constant 1.4 and 2.8 MHz. The inset shows the CW EPR spectrum of the radical at room temperature.

TABLE 1: Hyperfine Coupling Constants of Porphycene Anion Radical

cepstral peak designation	coupling constant determined from cepstrum, MHz	number of nuclei	type of nuclei	coupling constant from ENDOR, MHz[a]
a_A	0.5	2	H	+0.53
a_B	2.0	4	N	−2.00
a_C	2.5	4	H	−2.65
a_D	4.0	4	H	−4.10
a_E	4.6			
a_F	5.0	4	H	−5.05

[a] Ref 11.

Applications of Cepstral Analysis. *(1) Anthraquinone Anion Radical.* The anion radical of anthraquinone is a simple free radical with two sets of 4 equivalent protons. The hyperfine couplings of these two sets are in the ratio of 1:2 in this solvent and it should present a challenge to cepstral analysis. A cepstrum was generated from the quadrature free induction decay obtained after a $\pi/2$ microwave pulse.

The cepstrum of anthraquinone anion radical is shown in Figure 6A. Two positive peaks are clearly identified at 1.4 and 2.8 MHz, and another peak around 4.2 MHz is not so clearly seen. By seeing the two positive peaks at 1.4 and 2.8 MHz, one may be tempted to assign the 1.4 MHz coupling to a spin-1 nucleus. However, since the radical has two groups of 4 equivalent protons, we assigned the peak at 1.4 MHz to one group of 4 equivalent protons. The cepstrum was generated for a proton hyperfine coupling constant of 1.4 MHz and is shown in Figure 6C. This shows that the second cepstral peak of this coupling will be negative and its intensity will be half of the first peak. So the positive peak of Figure 6A at 2.8 MHz is a superposition of the second harmonic of 1.4 MHz coupling and the first harmonic of a 2.8 MHz coupling. This is because the two groups of nuclei have the same number of protons. The cepstrum corresponding to 2.8 MHz coupling to a proton is generated and shown in Figure 6B. By comparing the two synthesized cepstra with the experimental one, we see that three peaks are matching reasonably well and the coupling constants were determined in this case of accidental degeneracy between the two coupling constants. The finding, that the magnitude of one coupling constant is two times that of the other, is consistent with the CW spectrum of the radical showing 13 hyperfine lines.

(2) Porphycene Anion Radicals. The first derivative EPR absorption spectra of H_2PC1 and H_2PC2 anion radicals are shown in Figure 7. They consist of a large number of lines with few identifying features to enable one to recognize any but the smallest hyperfine coupling constant. From the structure of H_2PC1, we expect hyperfine couplings from 2 equivalent protons, 4 nearly equivalent nitrogens, and three groups of 4 equivalent protons.

The cepstrum of H_2PC1 is shown in Figure 8G. Since all the cepstral peaks are positive, identification of nuclei from the pattern of the peaks is impossible. We chose the peak position only to mark the coupling constants and their harmonics. We first chose the peak corresponding to the smallest coupling constant, a_A, and generated its cepstrum assuming it to be a proton coupling (Figure 8A). It appears that the first three peaks

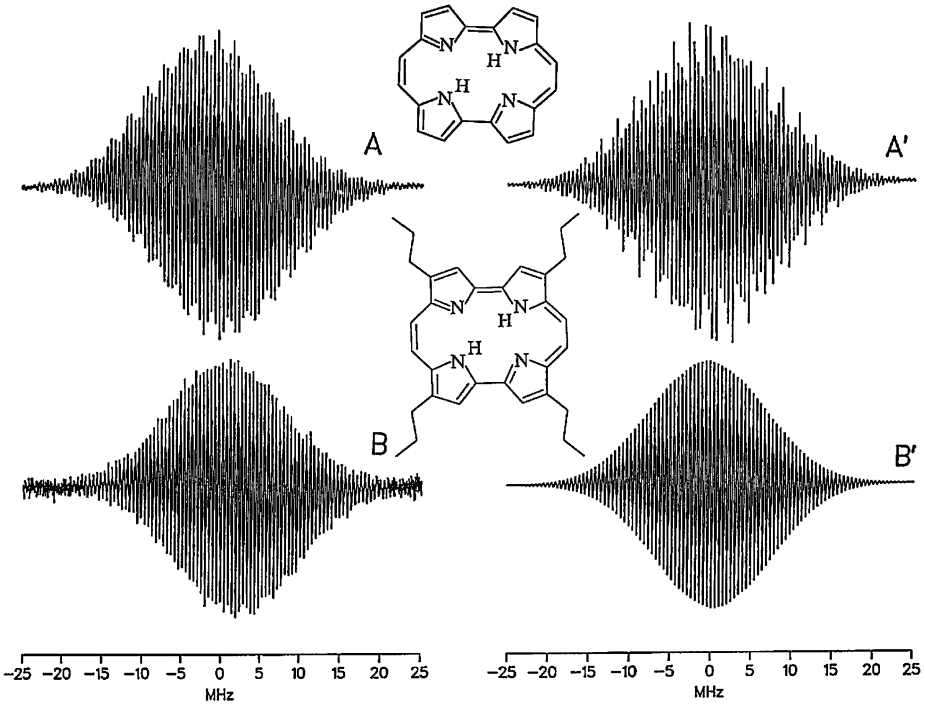

Figure 7. EPR spectra of porphycene anion radical (A) and tetrapropyl-porphycene anion radical (B) at 240 K. The center of the spectra at 0 MHz corresponds to the Zeeman field of 3242 G. (A′) and (B′) are spectra simulated using the hyperfine coupling constants determined from their cepstra. No attempt was made to optimize the coupling constants to improve the matching of the simulated spectra with the experimental spectra. The accuracy of the coupling constants obtained from the cepstral analysis was within 0.05 MHz. In the simulation reported by Schlüpmann et al.,[11] variations in the coupling constants needed to reproduce the experimental spectrum was less than this magnitude.

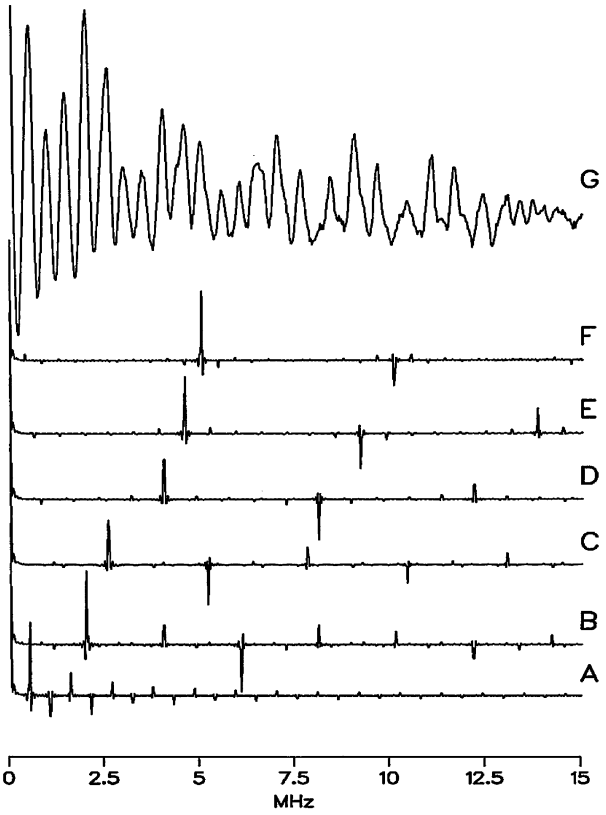

Figure 8. Cepstral analysis of the EPR spectrum of porphycene anion radical. (G) shows that cepstrum generated from the CW EPR spectrum shown in Figure 7(A). (A), (B), (C), (D), (E), and (F) show various simulated cepstra whose hyperfine couplings were identified from (G), as described in the text.

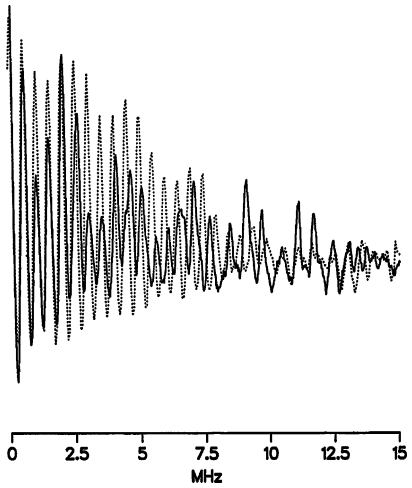

Figure 9. Comparison of cepstra of porphycene anion radical (−−) and tetrapropyl-porphycene anion radical (·····). The cepstra were generated from the corresponding EPR spectra shown in Figure 7.

of the cepstrum are the three harmonics of a_A. The fourth peak was taken to be another coupling constant, a_B. At this stage it was not known if this should be a nitrogen coupling. The fifth peak of the cepstrum with its intensity does not correspond to any harmonics of the earlier coupling constants. So it was chosen to be another coupling constant, a_C. In this way we found six possible coupling constants of which a_A, a_B, and a_C were unambiguously identified (see Table 1).

If a_i is the hyperfine coupling constant of a nucleus of spin I_i, the spectral width —the separation between the two outermost lines in its EPR spectrum—will be $2a_iI_i$ and the total width will be $\Sigma_i 2a_iI_i$. Thus the expected width for the three coupling constants, a_A, a_B, and a_C is at least 19 MHz, assuming that all three were due to proton nuclei. It was, therefore, not necessary to look for cepstral peaks with coupling constants greater than, say, 7 MHz, since the total spectral width would be too large to correspond to the observed width. Then we simulated the

TABLE 2: Hyperfine Coupling Constants of Tetrapropyl-porphycene Anion Radical

cepstral peak designation	coupling constant determined from cepstrum, MHz	number of nuclei	type of nuclei	coupling constant from ENDOR, MHz[a]
a_A	0.5	2	H	+0.48
a_B	1.96	4	N	−1.98
a_C	2.45	4	H	−2.53
a_D	2.99	8	H	+2.95
a_E	3.96	4	H	
a_F	4.45			−4.41

[a] Ref 12.

EPR spectrum with various combination of coupling constants and equivalent sets of nuclei. By visual comparison of simulated $y_1(t)$ and $Y'(\omega)$ with their observed profiles, the possible set of coupling constants was identified. It should be pointed out here that, since a_D is exactly twice a_B, the cepstral peak corresponding to a_D was initially thought to be the second harmonic of a_B and was not considered in the simulation. But this way no satisfactory simulation was possible, and a_D was assumed to represent a genuine coupling. From similar observations, a_F was chosen and a_E was rejected. A good simulation could be achieved with the values shown in Table 1. The accuracy of the coupling constants measured from the cepstral peaks is better than 0.05 MHz. Better accuracy requires observation of the harmonics. The simulated first derivative CW EPR spectrum of H_2PC1 is shown in Figure 7A′.

The cepstrum of H_2PC2 has even fewer identifying features than that of H_2PC1. We assumed that the coupling constants of the nuclei in the ring of H_2PC2 should be very similar to those of H_2PC1. Since one ring proton was replaced by the propyl chain, one proton coupling constant should be absent compared to H_2PC1. In Figure 9 the cepstra of H_2PC1 and H_2PC2 are superimposed to look for any difference in coupling constant. The values of the coupling constants of the ring protons and the nitrogen nuclei were measured from the cepstrum of H_2PC2 by comparing the respective peaks with those of H_2PC1. We did not have any knowledge of which proton hyperfine coupling constant in H_2PC1 would be absent in H_2PC2 because of propyl substitutions in the latter. So simulations were done assuming every possibility. But no simulation consisting of only the ring protons and the nitrogens would reproduce the observed spectrum. Only after the inclusion of couplings due to the methylene protons of the four propyl chains, which are close to the ring, could a good match be obtained. However, this way we identified two coupling constants, a_E and a_F (see Table 2), *both* of which produced simulated spectra visually indistinguishable from the experimental spectrum within the noise level. Using a set of 8 equivalent protons and its coupling constant to be a_E or a_F, we could obtain simulated $y_1(t)$ and $Y'(\omega)$ that matched very well with their respective experimental profiles. On comparison with the coupling constants from ENDOR, a_F was seen to represent the true coupling constant. In the absence of ENDOR data, a rigorous least-square fit of the experimental spectrum with the simulated signal could be used to choose between a_E and a_F. We did not attempt to do this, as this would be outside the main objective of the present work. The coupling constant a_E was used in the simulated spectrum in Figure 7B′.

The cepstral analysis of the porphecene radicals was done without any prior knowledge of the hyperfine coupling constants obtained from ENDOR spectroscopy. When the ENDOR data were available, we found that the cepstral analysis was less effective on the H_2PC2 anion radical signal than on the H_2PC1 anion signal. This technique correctly identified all the ENDOR-derived coupling constants of H_2PC1 and four coupling constants of H_2PC2. Even though the coupling constant a_F of H_2PC2 matches very well with the ENDOR data, our inability to choose between a_E and a_F is largely due to the poor signal-to-noise ratio of the spectrum. The root-mean-square error in the coupling constants measured from the cepstral peaks versus ENDOR was only 0.08 MHz for H_2PC1 and 0.21 MHz for H_2PC2 using a_E as the fifth coupling and 0.05 MHz using a_F as the fifth coupling.

Conclusion

Cepstral analysis has been useful in the analysis of complex EPR spectra of porphycene radical anions. Because of the finite signal-to-noise ratio, the cepstra alone do not offer enough information to make a complete analysis. However, when combined with the chemical structure, simulation of the EPR spectrum and simulation of the FID, cepstral analysis with thresholding is shown to be a powerful method of determining the hyperfine coupling constants and the number of equivalent nuclei. This technique will not replace ENDOR, particularly since well-resolved hyperfine splittings are required in the EPR spectrum. Nevertheless, it is a valuable adjunct to ENDOR, when an ENDOR spectrometer is not available, when the conditions for a measurable ENDOR response cannot be achieved, or when additional information about the numbers of equivalent nuclei is needed.

The anthraquinone and the porphycene radical anions investigated here provide a good test of cepstral analysis. They have no (or small) second-order shifts and nearly equal line widths, and they match the assumptions underlying cepstral analysis. Nevertheless, the spectra are not highly resolved, the weaker lines in some cases are lost in the noise, and several of the coupling constants are multiples of each other. Even under the worst conditions, the cepstra provided six possible hyperfine couplings, five of which agreed with the values obtained from ENDOR. Simulations of EPR spectra, the FID, and the cepstra allowed the assignment of the possible couplings to sets of protons and nitrogens in the radical, along with the numbers of equivalent nuclei involved.

Conditions for recording the EPR spectra to be used in the cepstral analysis are less stringent than in ENDOR where the solvent, the temperature, and the microwave power often need to be carefully optimized to record a useful ENDOR spectrum. We expect cepstral analysis to be a valuable aid in the interpretation of resolvable EPR spectra of organic radicals when the underlying assumptions of cepstral analysis are met.

Acknowledgment. H.L. is most grateful for his collaborations with Professor E. Vogel. The authors are all appreciative of the availability of CW EPR spectra of the porphycenes previously reported[11,12] and thank Mr. K. Hasharoni for providing the CW EPR spectra appropriate for cepstral analysis. This research was supported by the U.S. Department of Energy, Office of Basic Energy Sciences, Division of Chemical Sciences, under Grant DE-FG02-96ER14675 to J.R.N.

References and Notes

(1) Bogert, B. P.; Healy, M. J. R.; Tukey, J. W. In *Proceedings of the Symposium on Time Series Analysis*; Rosenblatt, M., Ed.; John Wiley: New York, 1963; Chapter 15.

(2) Kirmse, D. W. *J. Magn. Reson.* **1973**, *11*, 1.

(3) Möbius, K.; Plato, M.; Lubitz, W. *Phys. Rep.* **1982**, *87*, 171.

(4) Pearson, G. A.; Rocek, M.; Walter, R. I. *J. Phys. Chem.* **1978**, *82*, 1185.
(5) Vogel, E.; Köcher, M.; Schmickler, H.; Lex, J. *Angew. Chem., Int. Ed. Engl.* **1986**, *25*, 257.
(6) Dunham, W. R.; Fee, J. A.; Harding, L. J.; Grande, H. J. *J. Magn. Reson.* **1980**, *40*, 351.
(7) Dwight, H. B. In *Tables of Integrals and Other Mathematical Data*, 3rd ed.; Macmillan: New York, 1957; Equation 603.2.
(8) Angerhofer, A.; Massoth, R. J.; Bowman, M. K. *Israel J. Chem.* **1988**, *28*, 227.
(9) Bowman, M. K. In *Modern Pulsed and Continuous-wave Electron Spin Resonance*; Kevan, L., Bowman, M. K., Eds.; John Wiley: New York, 1990; Chapter 1.
(10) Massoth, R. J. Ph.D. Dissertation, University of Kansas, Lawrence, Mo., 1987.
(11) Schlüpmann, J.; Huber, M.; Toporowicz, M.; Köcher, M.; Vogel, E.; Levanon, H.; Möbius, K. *J. Am. Chem. Soc.* **1988**, *110*, 8566.
(12) Schlüpmann, J.; Huber, M.; Toporowicz, M.; Plato, M.; Köcher, M.; Vogel, E.; Levanon, H.; Möbius, K. *J. Am. Chem. Soc.* **1990**, *112*, 6463.